ACR No. L5C08

NATIONAL ADVISORY COMMITTEE FOR AERONAUTICS

WARTIME REPORT

ORIGINALLY ISSUED

April 1945 as
Advance Confidential Report L5C08

WIND-TUNNEL INVESTIGATION OF EFFECTS OF A PUSHER

PROPELLER ON LIFT, PROFILE DRAG, PRESSURE

DISTRIBUTION, AND BOUNDARY-LAYER

TRANSITION OF A FLAPPED WING

By Carl A. Sandahl

Langley Memorial Aeronautical Laboratory
Langley Field, Va.

NACA

WASHINGTON

NATIONAL ADVISORY COMMITTEE FOR AERONAUTICS

ADVANCE CONFIDENTIAL REPORT

WIND-TUNNEL INVESTIGATION OF EFFECTS OF A PUSHER

PROPELLER ON LIFT, PROFILE DRAG, PRESSURE

DISTRIBUTION, AND BOUNDARY-LAYER

TRANSITION OF A FLAPPED WING

By Carl A. Sandahl

SUMMARY

Some of the effects of pusher-propeller operation on
the aerodynamic characteristics of a flapped wing were
measured in the Langley propeller-research tunnel. The
effects of propeller operation on the lift and profile
drag of the wing, on pressure distribution, and on the
position of boundary-layer transition were obtained. The
results indicated that, at fixed angles of attack and with
flaps deflected, the wing lift increased appreciably with
increasing thrust coefficient. With flaps retracted, no
appreciable increase in lift with increases in thrust coef-
ficient was measured. Chordwise pressure distributions at
several spanwise stations indicated that the effect of
propeller operation was greatest in the region immediately
ahead of the propeller and that the effect extended out-
board from the propeller axis for about 2.5 propeller radii.
Measurements of boundary-layer velocity on the forward part
of the upper surface of the wing showed no appreciable
shift of transition in the range of thrust coefficients
investigated.

INTRODUCTION

As part of a study of the efficiency of a pusher
propeller behind a low-drag wing, some measurements
relating to the effects of the propeller inflow on the
aerodynamic characteristics of the wing were made in the
Langley propeller-research tunnel. The data, which are
presented herein, show the effects of propeller operation

on the lift of the wing with flaps retracted and deflected, on the pressure distribution, on the section profile drag, and on the position of boundary-layer transition on the upper surface.

APPARATUS AND TESTS

The general arrangement of the model used in the present investigation is shown in figure 1 and the model configurations, in figure 2. The geometric character- istics of the model are as follows:

Wing area with flap retracted, square feet 77.27
Wing span, feet 16.06
Wing chord with flap retracted, feet 4.932
Aspect ratio 3.34
Airfoil section . . . . NACA 63,4-420 (approx.)
Flap chord, feet 1.32
Propeller diameter, feet 4.0

The wing was constructed of wood covered with fiber- board. For the tests to determine boundary-layer transi- tion, the wing was carefully sanded and waxed; however, for the other tests, including the measurements of profile drag, the wing was considerably less smooth, particularly at the leading edge. Full-span landing flaps of single- slotted, double-slotted, and split types were used with the wing. The nacelle was faired into the wing and no provision was made for air flow through the nacelle.

The three-blade propeller with a 4-foot diameter was a Hamilton-Standard 6101 design of modified pitch distribution and right-hand rotation. (See fig. 3.) The propeller was driven by a variable-speed variable-frequency induction motor rated at 70 horsepower at 3000 rpm. The propeller blades were set at 22.5° at the 0.75-radius station. The maximum propeller rotational speed was 3000 rpm, and the maximum wind-tunnel speed was 80 miles per hour. Tunnel speeds lower than the maximum were necessary in developing the higher values of thrust coefficient of these tests. The range of thrust coefficients used was extended to values considerably higher than those of normal flight in order to accentuate the effects of propeller operation on the aerodynamic characteristics of the wing.

Lifts were measured over a range of thrust loadings at flap deflections of 0°, 20°, and 40° and at geometric angles of attack of 0°, 3°, 6°, and 9°. Pressure distribution, profile drag, and boundary-layer transition were measured only with the flap retracted.

The section profile-drag coefficient was measured at three spanwise stations in the vicinity of the propeller. (See fig. 1.) The limited space between the wing and the propeller necessitated mounting the rake immediately behind the trailing edge as shown in figure 4. Both static and total pressure were measured.

The pressure distribution over the wing was measured with a pressure belt constructed of 0.040-inch copper tubes soldered together as shown in figure 5. The excess solder was scraped from the surface of the belt, and an orifice with a diameter of 0.020 inch was drilled into the wall of each tube at the desired chordwise locations. The belt was then formed to the wing section and mounted on the surface.

Boundary-layer transition was determined from measurements in the boundary layer over the forward 60 percent of the upper surface of the wing at seven spanwise stations. (See fig. 1.) The total pressure in the boundary layer was measured with 0.040-inch stainless steel tubes flattened to an inside height of 0.006 inch. (See fig. 6.) The geometric centers of the tubes were set 0.011 inch above the wing surface. The velocity in the boundary layer was calculated by using the total pressure in the boundary layer and the local static pressure previously measured with the pressure belt.

SYMBOLS

C_{L_T} total lift coefficient of wing with propeller operating $\left(\dfrac{\text{Resultant vertical force}}{q_0 S}\right)$

ΔC_{L_p} increment of lift coefficient due to propeller thrust inclination

$$\left(\dfrac{\text{Vertical component of propeller axial force}}{q_0 S} = \dfrac{T_e \sin \alpha}{q_0 S}\right)$$

C_L net lift coefficient of wing $\left(C_{L_T} - \Delta C_{L_p}\right)$

c_{d_o} section profile-drag coefficient

$$\left(\frac{\text{Section profile drag}}{q_o c}\right)$$

T_c effective thrust disk-loading coefficient based

on propeller disk area $\left(\dfrac{T_e}{\rho V_o^2 D^2}\right)$

T_e effective thrust, pounds

D propeller diameter, feet

V_o free-stream velocity, feet per second

u velocity in surface direction inside boundary
       layer, feet per second

S wing area, square feet

c wing chord, feet

ρ mass density of air, slugs per cubic foot

α angle of attack, degrees; measured between thrust
       line (coincident with chord line) and relative
       wind; corrected for jet boundary

δ_f flap deflection, degrees

x distance from leading edge of wing parallel to
       chord line

y lateral distance from plane of symmetry

q_o free-stream dynamic pressure $\left(\frac{1}{2}\rho V_o^2\right)$

p local static pressure on wing

p_o free-stream static pressure

$\overline{P}$ average chordwise pressure ratio $\left(\dfrac{p - p_o}{q_o}\right)$

RESULTS AND DISCUSSION

The results of this investigation are presented in four sections showing the effects of propeller operation on (1) lift, (2) chordwise and spanwise pressure distribution, (3) boundary-layer transition, and (4) profile drag. The data are expressed in nondimensional coefficients and have been corrected for jet-boundary effects.

In a preliminary comparison, it was found that lift with propeller operating at $T_c = 0$ would agree with lift for the propeller removed within experimental accuracy. The lift coefficients at $T_c = 0$ in this report may therefore be considered as propeller-removed values.

Effect of propeller operation on lift.- Lift with power on is considered to have four components: (1) the lift of the wing at $T_c = 0$, (2) the increment of lift of the wing caused by operation of the propeller, (3) the vertical component of propeller axial force, and (4) the propeller normal force. The maximum propeller normal force developed in these tests is estimated to be within the scatter of experimental points. Component (2), the increment of lift, is then obtained by deducting components (1) and (3) from the measured resultant vertical force. In evaluating component (3), the propeller axial force was assumed to be equal to the effective thrust and independent of angle of attack at a given value of advance-diameter ratio.

The variation of total lift coefficient C_{L_T} with thrust disk-loading coefficient T_c is given in figure 7 for several angles of attack and several flap deflections. In correcting the angles of attack for jet-boundary effects, the total lift coefficient C_{L_T} at $T_c = 1.0$ was used. This simplification introduced inaccuracies in angle of attack of the order of $\pm 0.3^\circ$ and corresponding changes in total lift coefficient of ± 0.012, which is within the scatter of the experimental points. The vertical component of propeller axial force has been

deducted from the faired curves of total lift coefficient
of figure 7, and the resulting net lift coefficient is
cross-plotted against angle of attack at three values
of T_c in figure 8. In this figure, the angle of attack
has been corrected by using the total lift coefficient
at each value of T_c. The curves of figure 8 indicate
that the slope of the lift curve is approximately
independent of T_c. With flaps retracted, propeller
operation - even at high thrust coefficients - did not
appreciably affect the wing lift (fig. 8(a)). With
flaps deflected, however, the lift increased with
increasing T_c. The increment of wing lift resulting
from propeller operation is the difference in lift
between the curves for $T_c = 0$ and curves for the
propeller operating in figure 8 and is attributed to
only the propeller inflow. It is noted that a British
investigation (reference 1) shows larger increases in
lift due to propeller operation than were measured in
the present investigation.

Less lift was obtained at $T_c = 0$ with the double
than with the single slotted flap. The difference may
have been caused by incorrect design of the double
slotted flap.

Effect of propeller operation on pressure distri-
bution.- The chordwise pressure distribution at several
spanwise stations and several values of T_c is given in
figure 9. The maximum observed decrease in local pres-
sure associated with propeller operation occurred near
the trailing edge at $\frac{y}{c} = 0.20$, the point of measure-
ment nearest the thrust center line. The pressure decrease
at $\delta_f = 0°$ was approximately the same over the upper
and lower surfaces, an indication that there was no
appreciable change in lift. This result is in agreement
with the results of the force tests given in figure 8(a).

From figure 10, in which the average chordwise pres-
sure ratio is plotted against spanwise station, it may
be noted that the propeller effect extended outboard to
$\frac{y}{c} \approx 1.0$, or about 2.5 propeller radii from the propeller
axis.

Effect of propeller operation on boundary-layer transition.- The ratio of the velocity at a constant height (0.011 in.) in the boundary layer to free-stream velocity u/V_0 is plotted as a function of the distance from the leading edge x/c in figure 11 for several thrust coefficients and test velocities. No appreciable shift in transition associated with propeller operation or with Reynolds number was measured. This result is in agreement with reference 2.

Effect of propeller operation on section profile drag.- The section profile-drag coefficient was measured at three spanwise stations in the vicinity of the propeller. (See fig. 1.) The variation of section profile-drag coefficient with thrust disk-loading coefficient is given in figure 12 for three test velocities. The rather high profile-drag coefficients measured at $T_c = 0$ are attributed to surface roughness near the leading edge, which presumably caused transition to occur much farther forward than with the highly polished surface on which the transition measurements of figure 11 were obtained. Larger increases of section profile-drag coefficient with increasing thrust coefficient occurred than can be accounted for as increased skin friction due to the increased velocity in the propeller inflow. These increases in drag coefficient are probably due to the action of the low-pressure region in front of the propeller in drawing low-energy boundary-layer air from other sections of the wing toward the sections ahead of the survey rake.

CONCLUSIONS

The foregoing analysis of measurements made to determine the effects of pusher-propeller operation on some of the aerodynamic characteristics of a low-drag wing with flaps indicated that:

1. At fixed angles of attack and with flaps deflected, the lift of the wing increased appreciably with increasing thrust coefficient.

2. Changes in pressure distribution over the wing caused by propeller operation were largest immediately ahead of the propeller and extended outboard to approximately 2.5 propeller radii from the propeller axis.

With flaps retracted, no appreciable change in wing lift
or span load distribution was measured.

3. No appreciable shift of transition with varia-
tion of thrust coefficient was measured.

Langley Memorial Aeronautical Laboratory
    National Advisory Committee for Aeronautics
        Langley Field, Va.

REFERENCES

1. Smelt, R., and Smith, F.: Note on Lift Change Due to
     an Airscrew Mounted behind a Wing. Rep. No. B.A.
     1514, British R.A.E., Dec. 1938, and Addendum,
     Rep. No. B.A. 1514a, April 1939.

2. Hood, Manley J., and Gaydos, M. Edward: Effects of
     Propellers and of Vibration on the Extent of
     Laminar Flow on the N.A.C.A. 27-212 Airfoil.
     NACA ACR, Oct. 1939.

Single slotted flap

Section A-A

Pressure-belt positions, y/c

Double slotted flap

.20
.45
.69
.93

Survey-rake positions, y/c

.60 .40 .20

59.18"

Split flap

15.79"

15.79"

40°

40°

40°

3.97"

5.95"

15.79"

".20 .30 .40 .51 .61 .71 .81 ← Boundary-layer tube positions, y/c

192.7"

180.0"

D = 48"

Chord plane

5.75"

NATIONAL ADVISORY
COMMITTEE FOR AERONAUTICS

Figure 1.- General arrangement of model.

Fig. 1
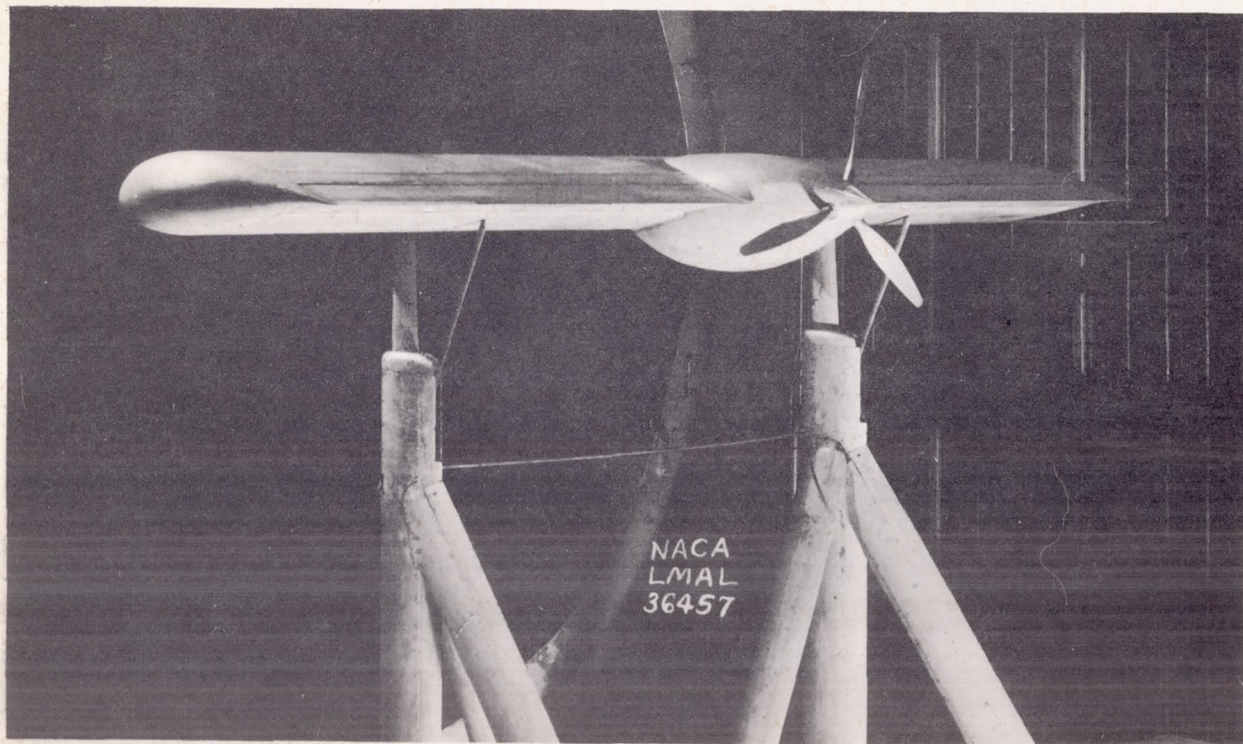
(a) Slotted flap retracted.

Figure 2.- Several configurations of model mounted in Langley propeller-research tunnel.

CONFIDENTIAL
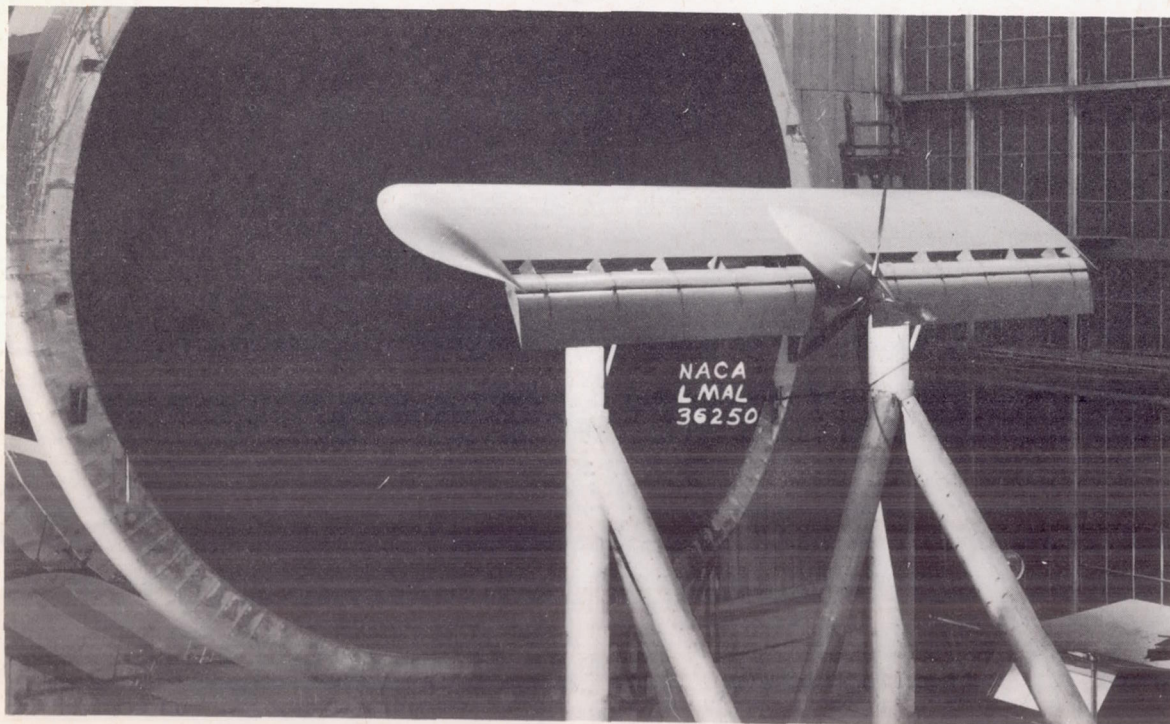
(b) Double slotted flap.

Figure 2.- Continued.

CONFIDENTIAL

(c) Split flap. The portion of the flap shown fitted on the nacelle
was not installed for these tests.

Figure 2.- Concluded.   CONFIDENTIAL

CONFIDENTIAL

Leading edge

Blade plan form (developed)

Spinner outline
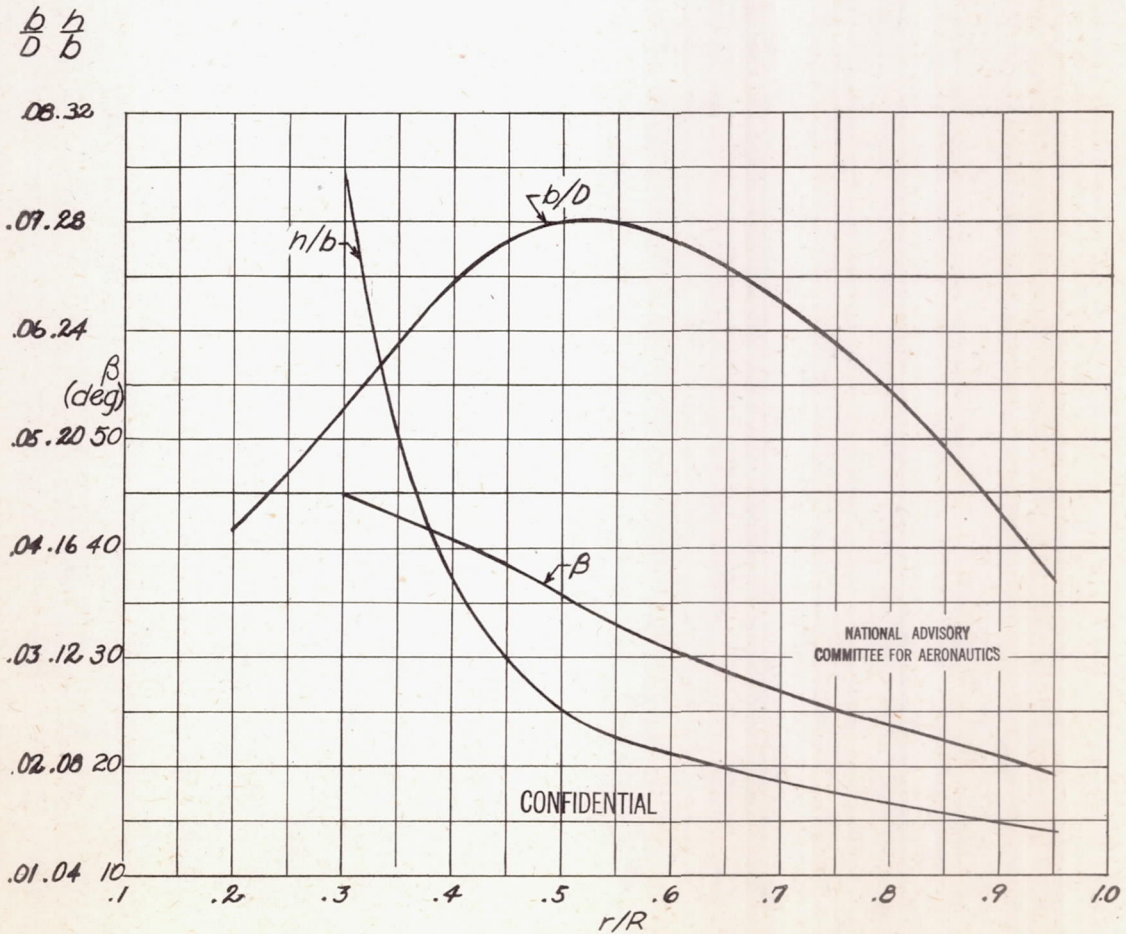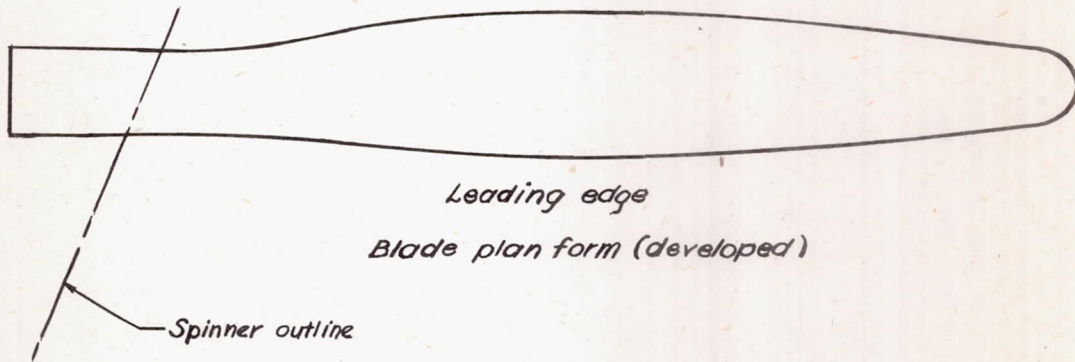
Figure 3.- Plan-form and blade-form curves for the modified Hamilton Standard 6101 propeller.
R, radius to tip; D, diameter; b, section chord; h, section thickness; r, station radius;
β, section blade angle.

CONFIDENTIAL
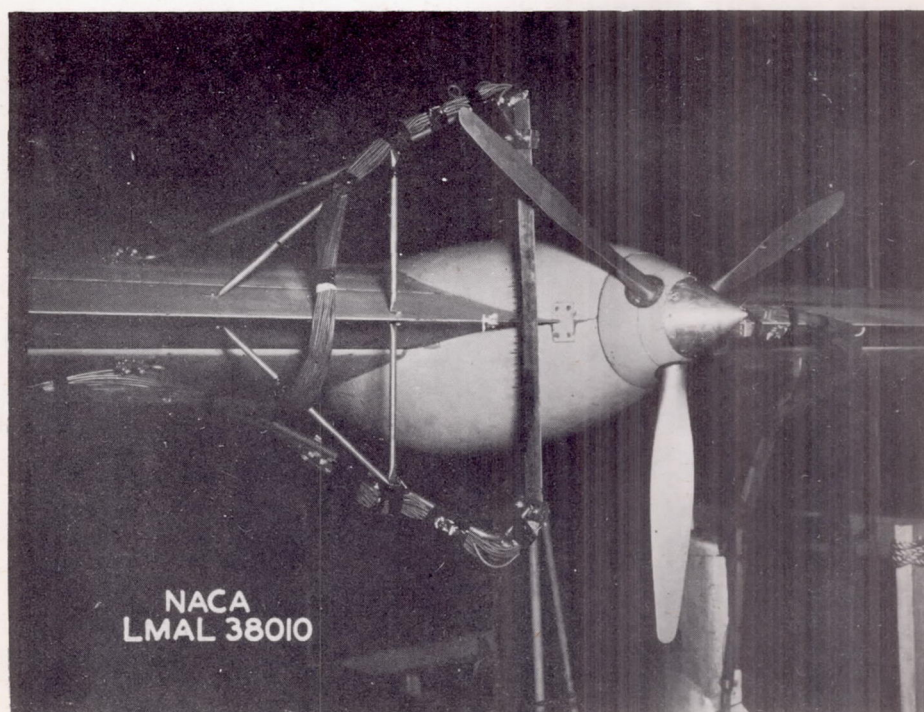
Figure 4.- Wake-survey rake installed between wing
trailing edge and propeller.
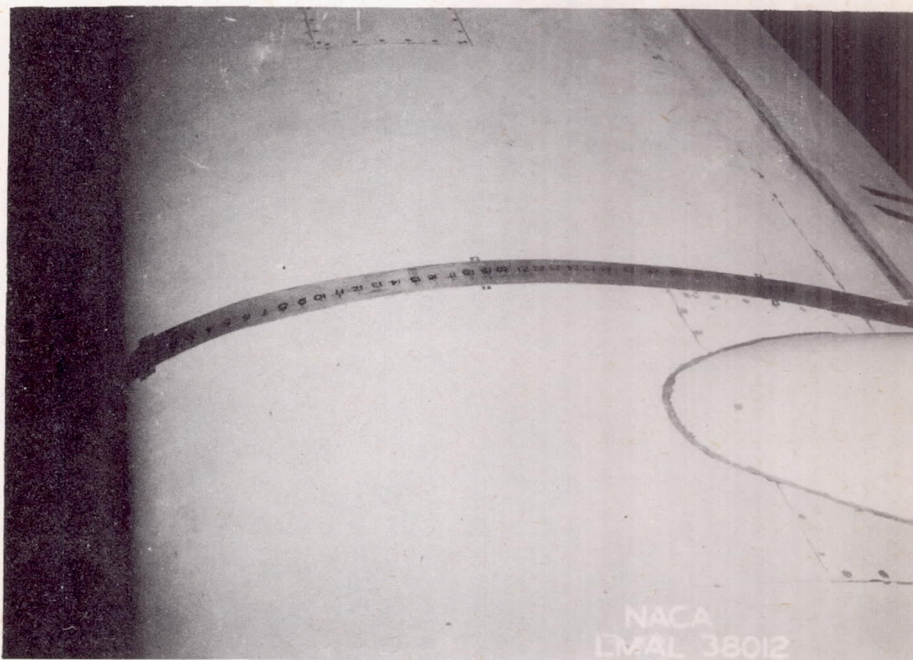
CONFIDENTIAL

Figure 5.- Pressure belt installed on wing.

Figure 6.- Boundary-layer total-pressure tube installed on wing.
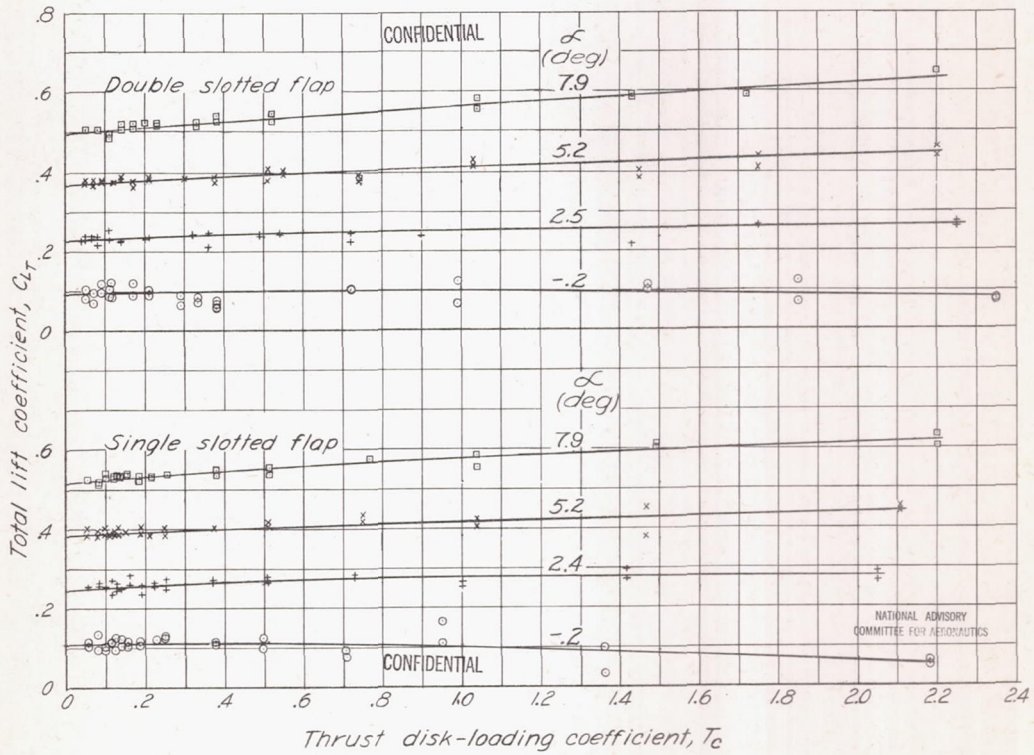
(a) $\delta_F, 0°$.

Figure 7.- Variation of total lift coefficient with thrust disk-loading coefficient
for single slotted, double slotted, and split flaps.

(b) δ_f, 20°.

Figure 7.- Continued

CONFIDENTIAL

α (deg)

Split flap

6.8

-1.2

α (deg)

Double slotted flap

6.5

3.8

-1.6

Single slotted flap

α (deg)

6.3

3.6

.9

-1.7

CONFIDENTIAL

NATIONAL ADVISORY
COMMITTEE FOR AERONAUTICS

Total lift coefficient, C_{L_T}

Thrust disk-loading coefficient, T_c
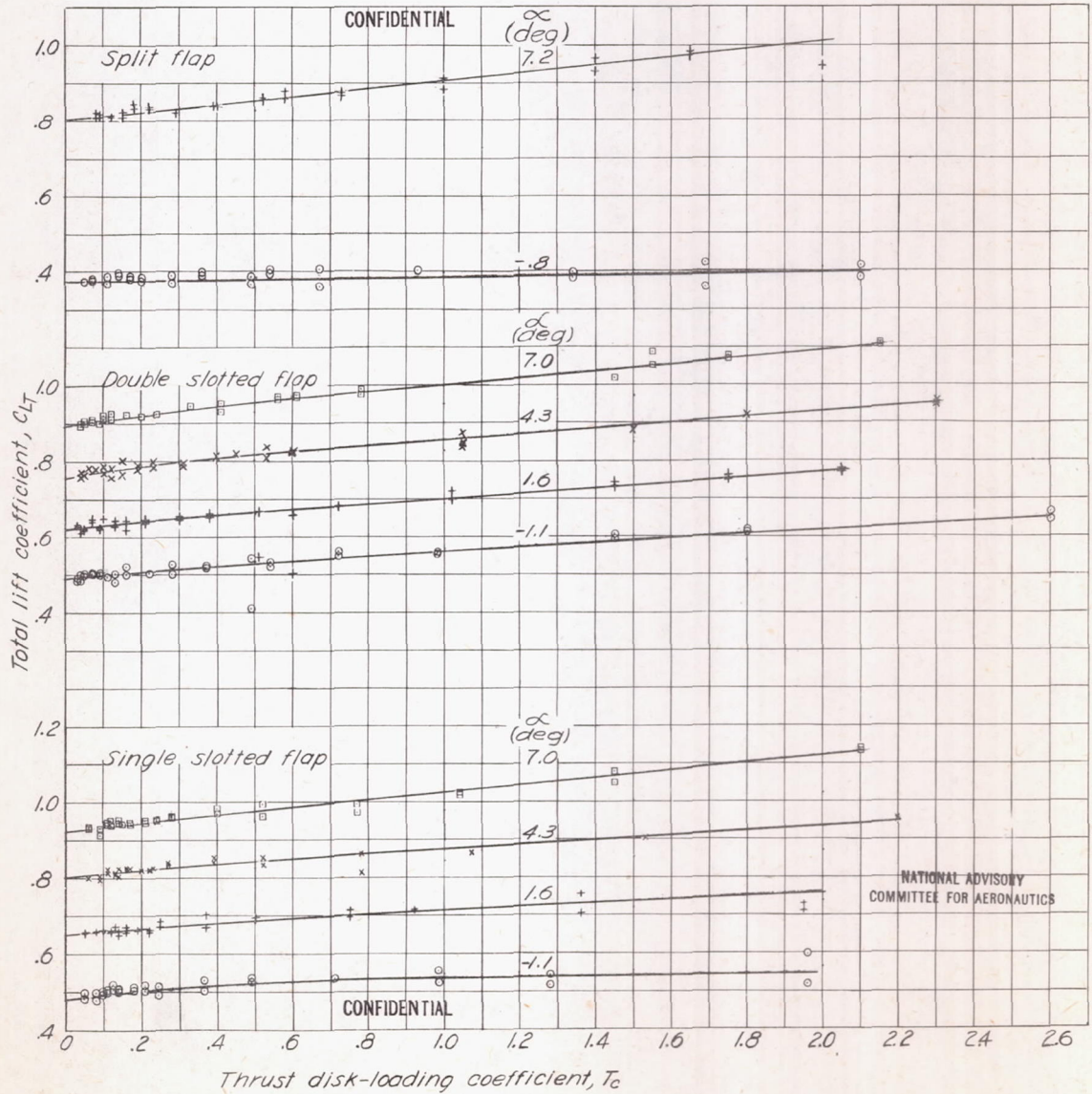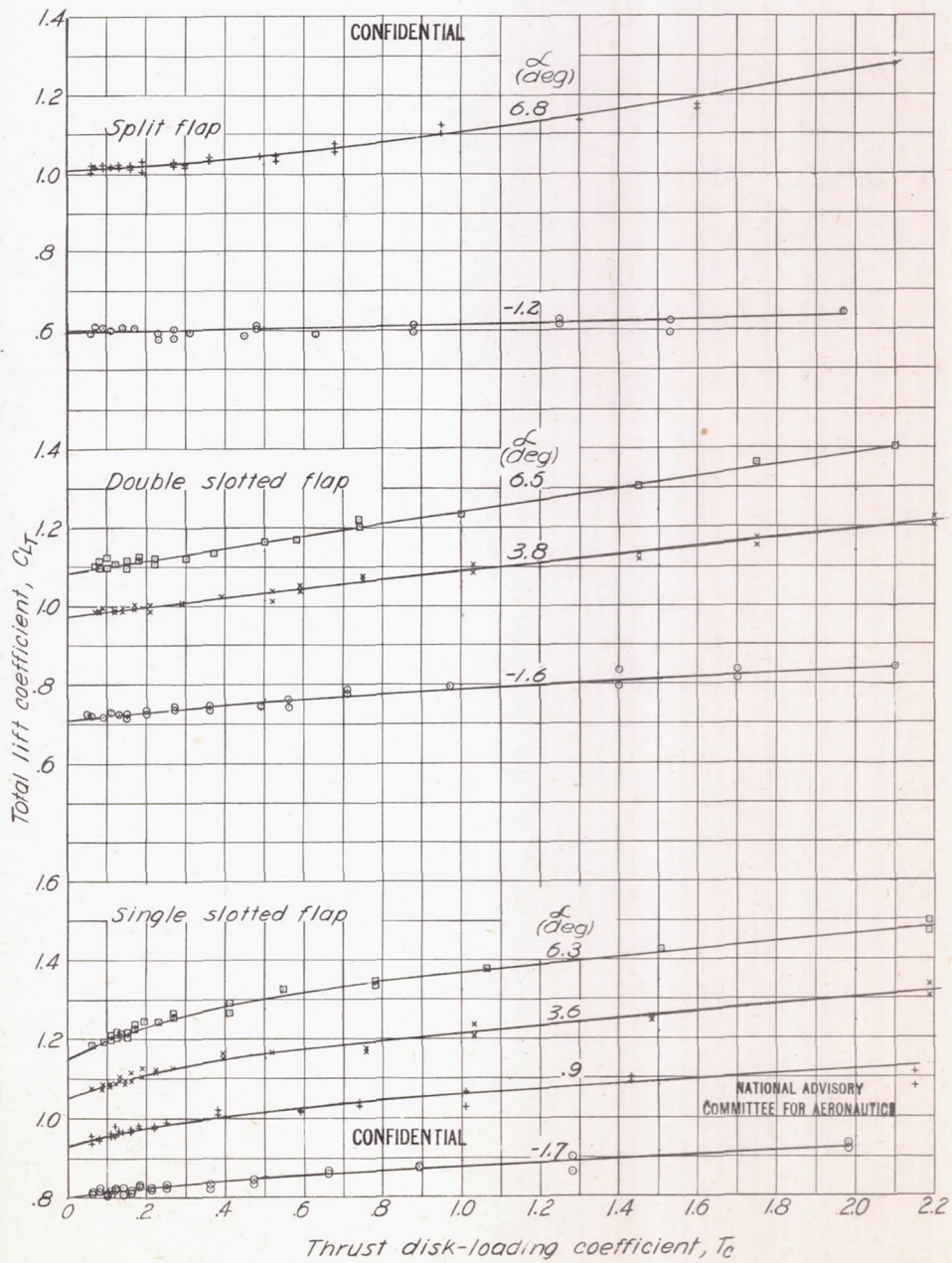
(c) δ_f, 40°.

Figure 7 .- Concluded.

(a) δ_f, 0°.   (b) δ_f, 20°.   (c) δ_f, 40°.
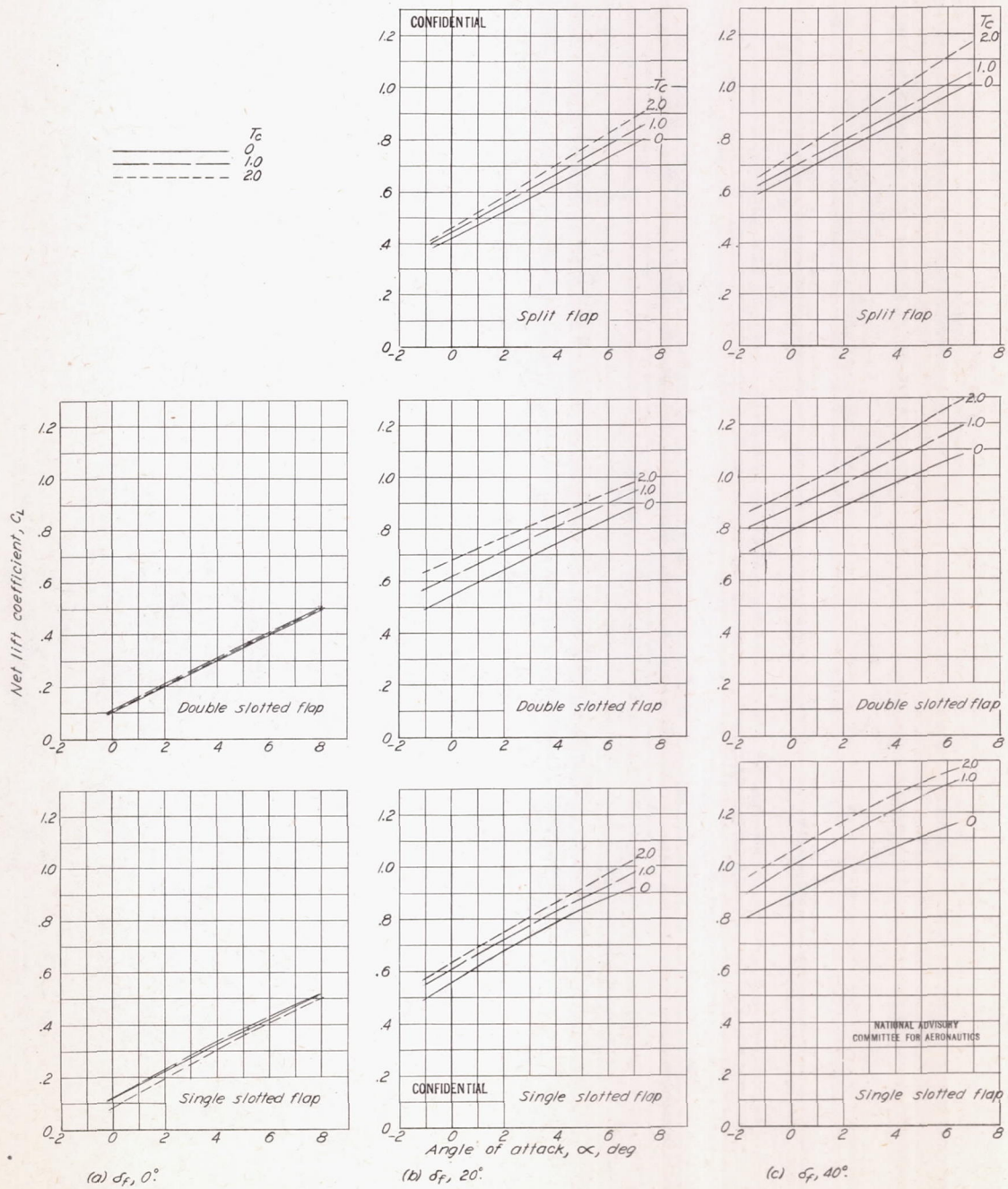
Figure 8.- Effect of T_c on variation of net lift coefficient with angle of attack.

Upper surface   CONFIDENTIAL   Spanwise station, y/c, 0.20   Lower surface

$\frac{p-p_0}{q_0}$

T_c
0 ○
.54 +
1.02 ×

Spanwise station, y/c, .45

$\frac{p-p_0}{q_0}$

T_c
0 ○
.53 +
1.00 ×

Spanwise station, y/c, .69

$\frac{p-p_0}{q_0}$

T_c
0 ○
.50 +
1.02 ×

Spanwise station, y/c, .93

$\frac{p-p_0}{q_0}$

T_c
0 ○
1.00 +

NATIONAL ADVISORY
COMMITTEE FOR AERONAUTICS

CONFIDENTIAL

Distance from leading edge, x/c

Distance from leading edge, x/c
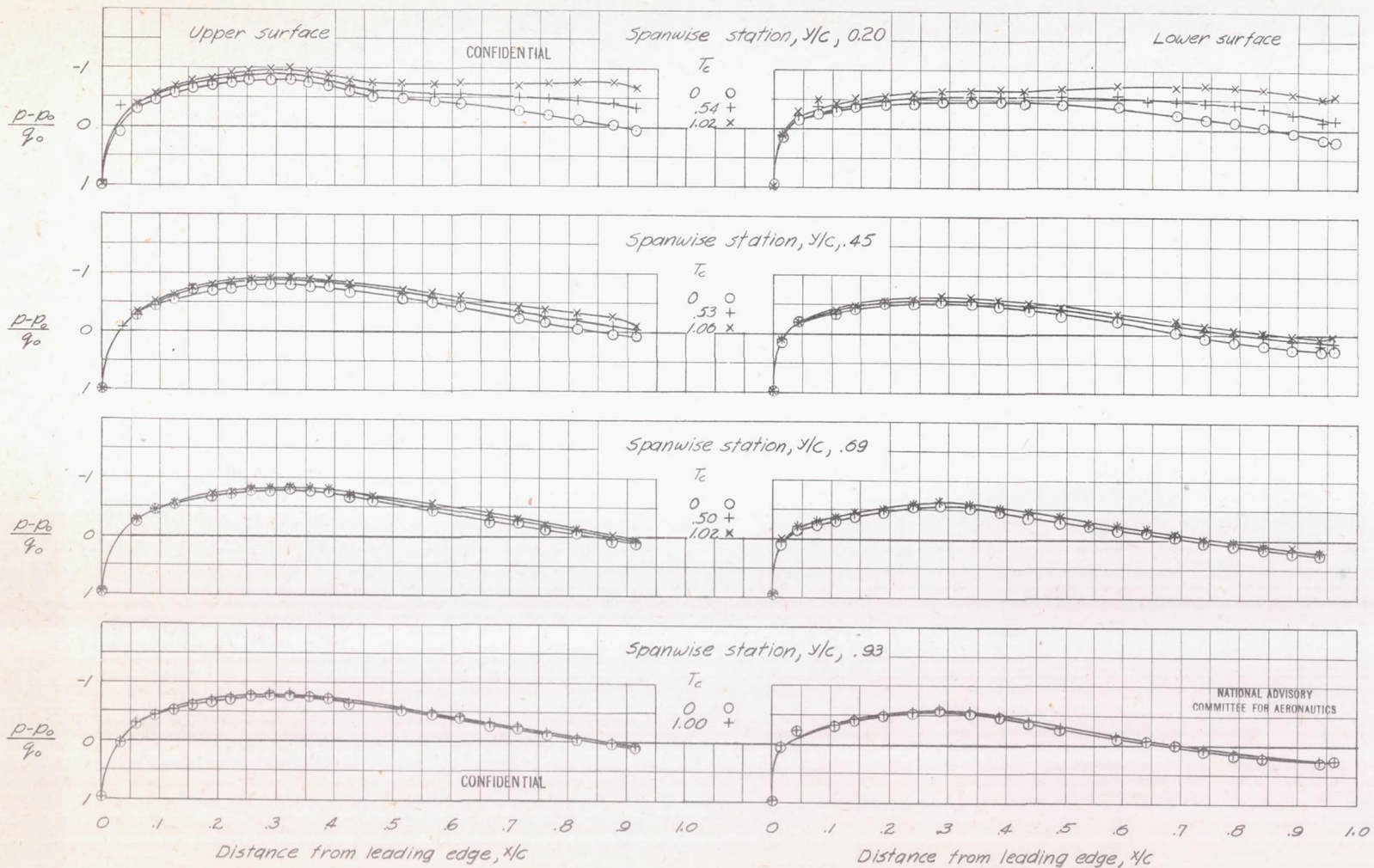
(a) α, -0.2°; C_L, 0.11.

Figure 9.- The chordwise pressure distribution at several spanwise stations. Single slotted flap; δ_f, 0°.

Upper surface   Spanwise station, y/c, 0.20   Lower surface

CONFIDENTIAL

T_c
0   0
.54   +
1.14   ×

$\dfrac{p-p_0}{q_0}$

Spanwise station, y/c, .45

T_c
0   0
.53   +
1.11   ×

$\dfrac{p-p_0}{q_0}$

Spanwise station, y/c, .69

T_c
0   0
1.06   +

$\dfrac{p-p_0}{q_0}$

Spanwise station, y/c, .93

T_c
0   0
1.11   +

NATIONAL ADVISORY
COMMITTEE FOR AERONAUTICS

CONFIDENTIAL

$\dfrac{p-p_0}{q_0}$

Distance from leading edge, x/c Distance from leading edge, x/c
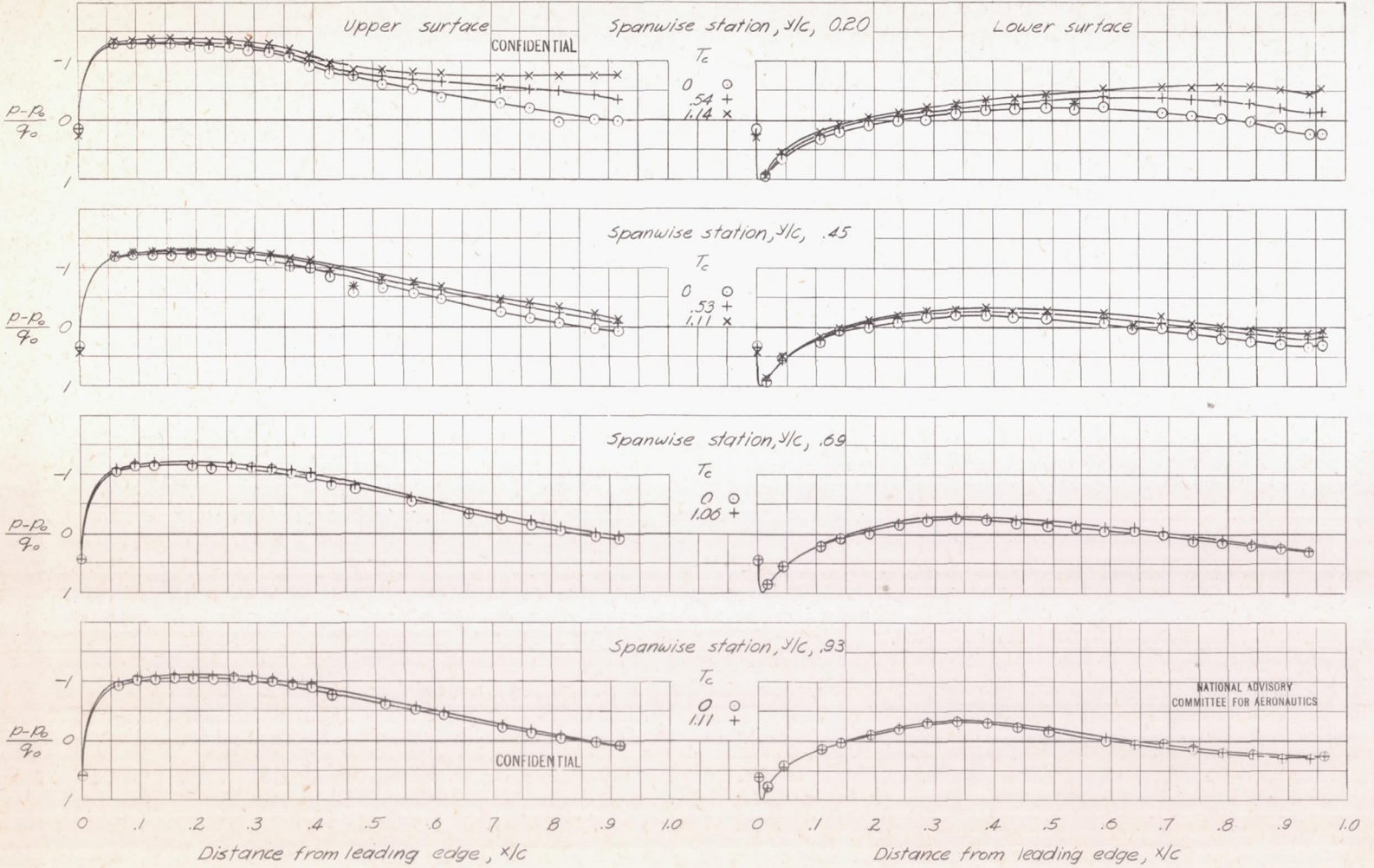
(b) α, 8.0°; C_L, 0.51.

Figure 9.- Concluded.

(a) α, 8.0°.

(b) α, - 0.2°.
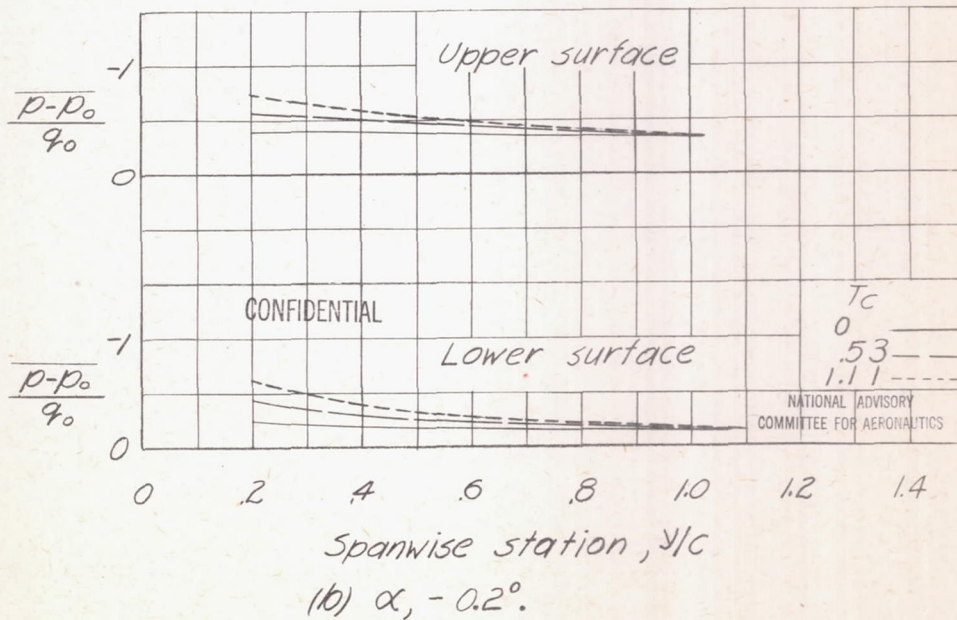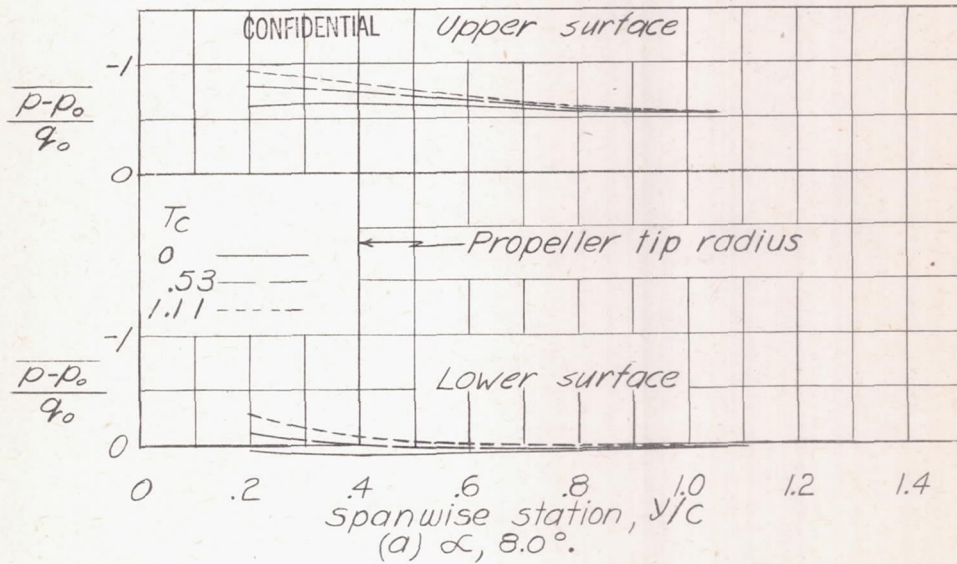
Figure 10.- Variation of average pressure over upper and lower surfaces with thrust coefficient. Single slotted flap; δ_f, 0°.
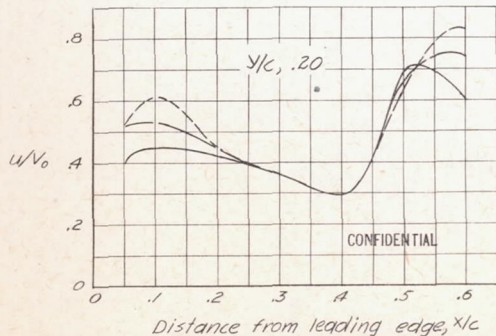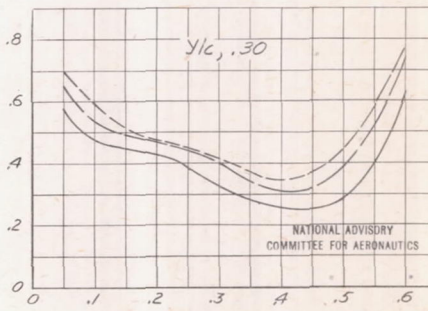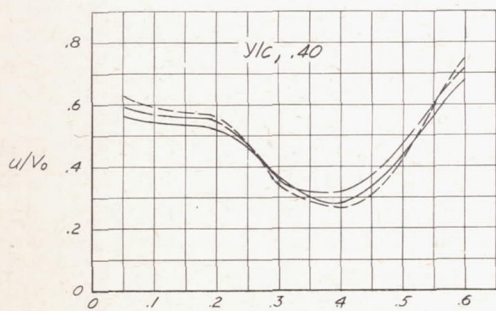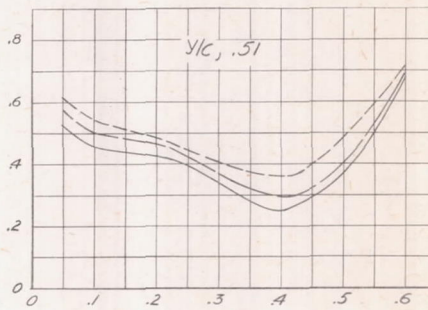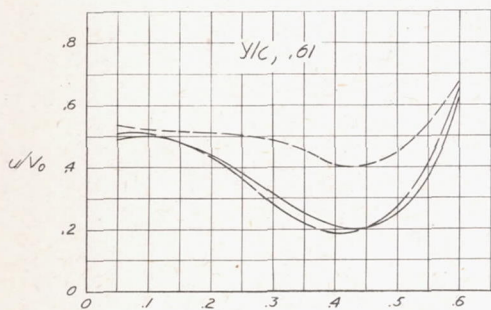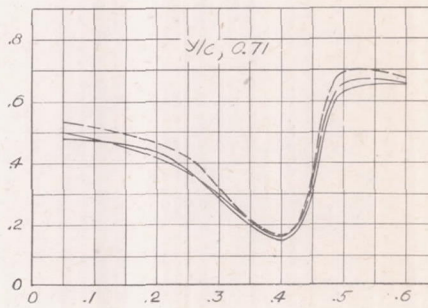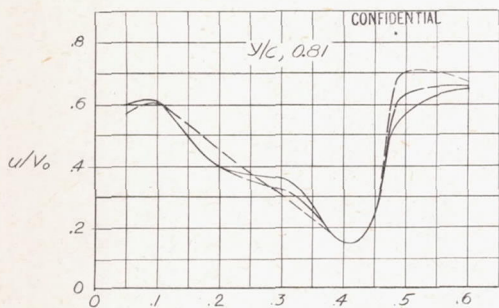
Figure 11.- Variation of boundary-layer velocity with distance from leading edge. Single slotted flap; δ_f, $0°$; α, $-0.2°$.
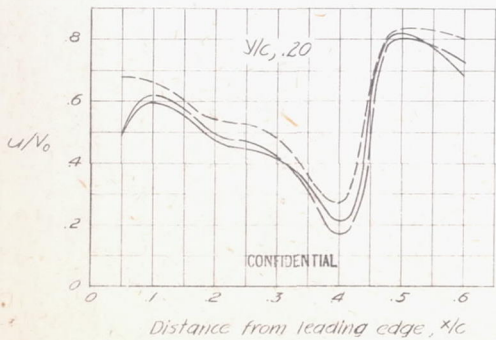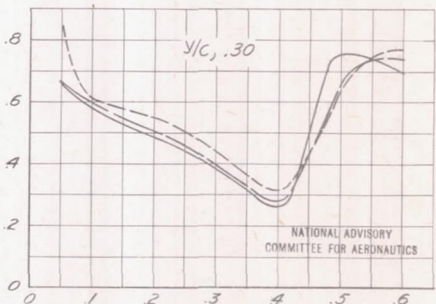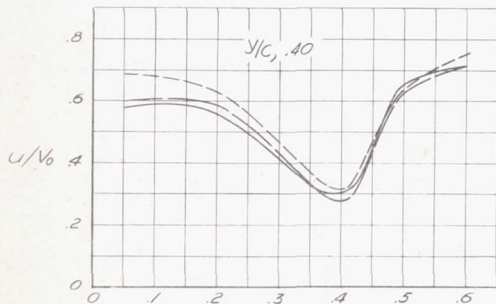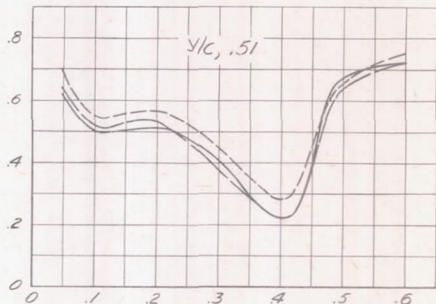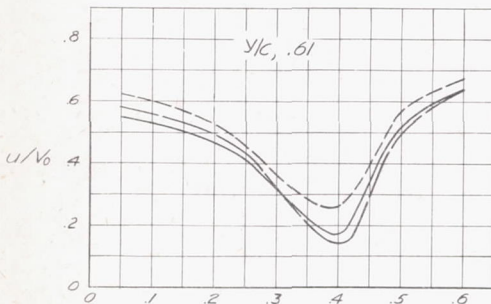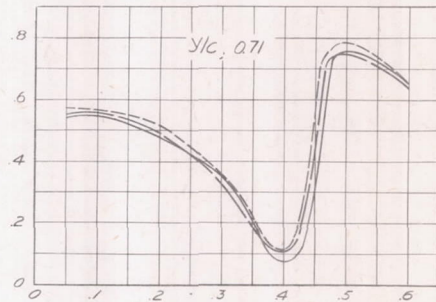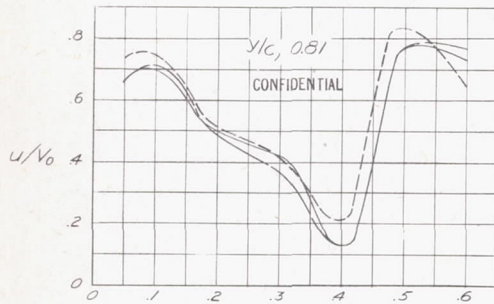
(a) V_0, 33 miles per hour (approx).

(b) V_0, 46 miles per hour (approx.).
Figure 11.- Continued.

(c) V_0, 60 miles per hour (approx).

Figure 11.- Concluded.
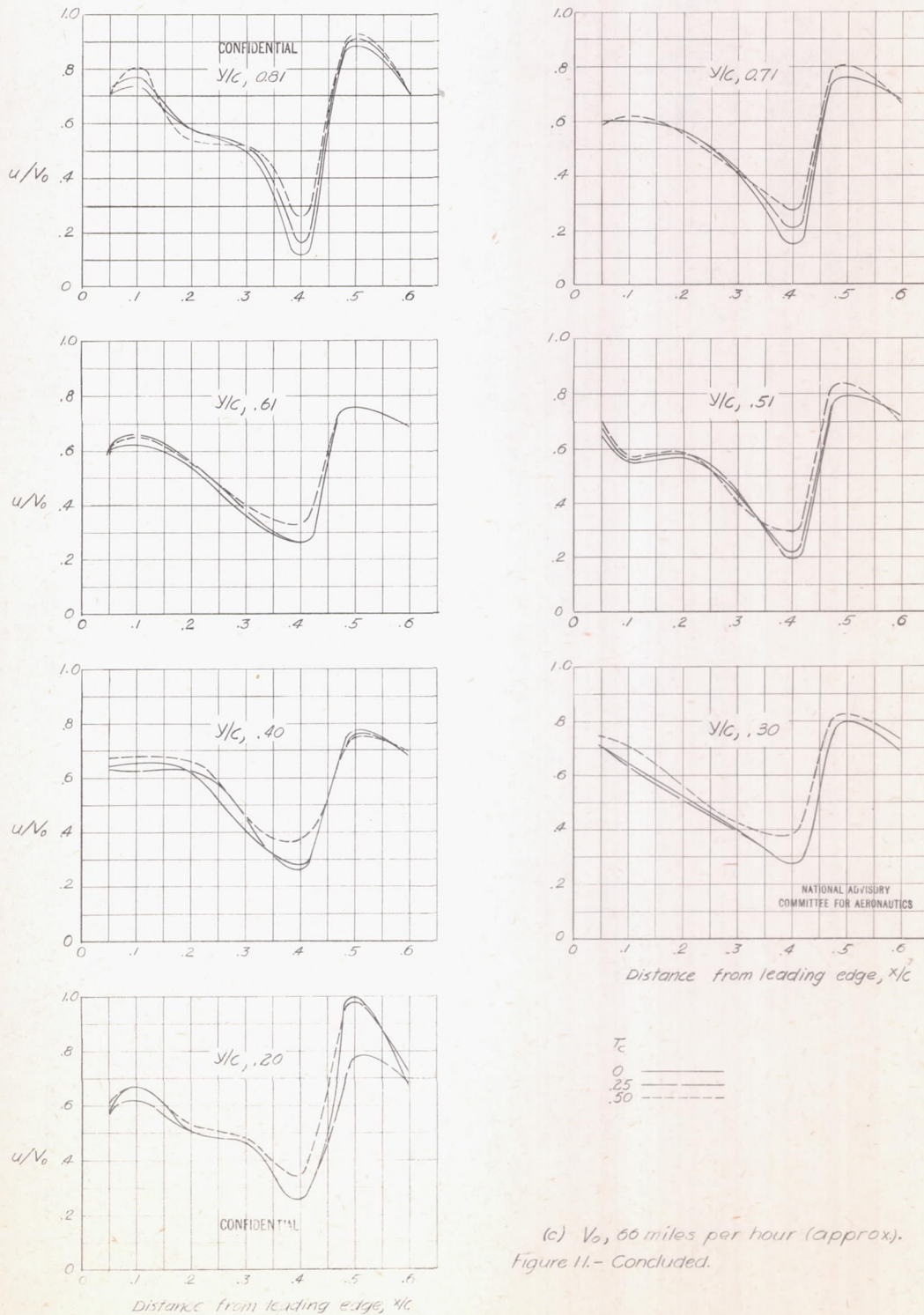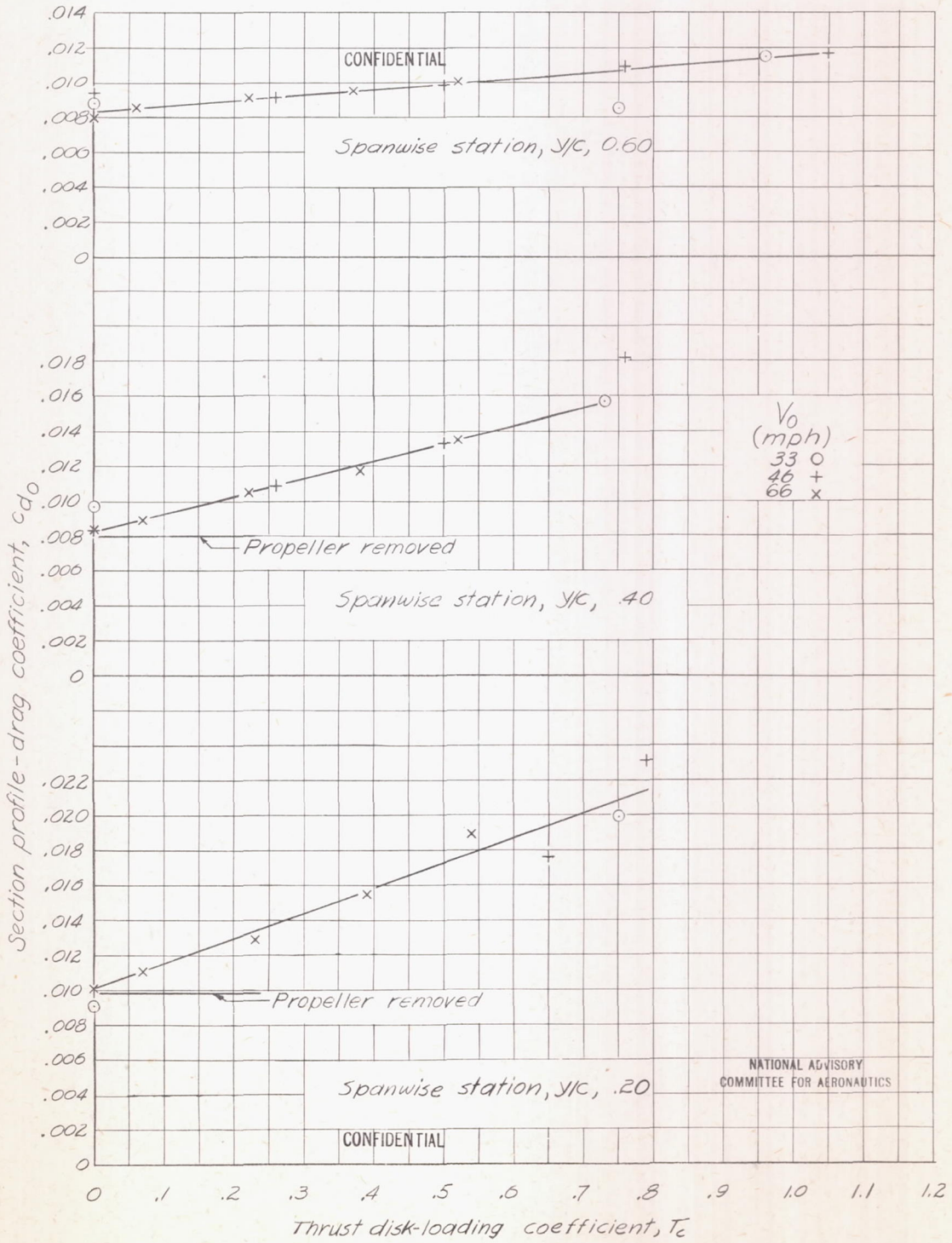
Figure 12.- Variation of section profile-drag coefficient with propeller thrust coefficient. Single slotted flap; d_f, 0°; α, -0.2°; c_L, 0.11.